



**HAL**  
open science

# Anisotropic collision-induced Raman scattering by the Kr:Xe gas mixture

Sophie Dixneuf, Michel Chrysos, Florent Rachtet

► **To cite this version:**

Sophie Dixneuf, Michel Chrysos, Florent Rachtet. Anisotropic collision-induced Raman scattering by the Kr:Xe gas mixture. *Journal of Chemical Physics*, 2009, 131 (7), Non spécifié. 10.1063/1.3200929 . hal-03420391

**HAL Id: hal-03420391**

**<https://univ-angers.hal.science/hal-03420391>**

Submitted on 9 Nov 2021

**HAL** is a multi-disciplinary open access archive for the deposit and dissemination of scientific research documents, whether they are published or not. The documents may come from teaching and research institutions in France or abroad, or from public or private research centers.

L'archive ouverte pluridisciplinaire **HAL**, est destinée au dépôt et à la diffusion de documents scientifiques de niveau recherche, publiés ou non, émanant des établissements d'enseignement et de recherche français ou étrangers, des laboratoires publics ou privés.

## Anisotropic collision-induced Raman scattering by the Kr:Xe gas mixture

S. Dixneuf, M. Chrysos, and F. Rachet

Citation: *The Journal of Chemical Physics* **131**, 074304 (2009); doi: 10.1063/1.3200929

View online: <http://dx.doi.org/10.1063/1.3200929>

View Table of Contents: <http://scitation.aip.org/content/aip/journal/jcp/131/7?ver=pdfcov>

Published by the [AIP Publishing](#)

---

### Articles you may be interested in

[Heavy rare-gas atomic pairs and the “double penalty” issue: Isotropic Raman lineshapes by Kr<sub>2</sub>, Xe<sub>2</sub>, and KrXe at room temperature](#)

*J. Chem. Phys.* **143**, 174301 (2015); 10.1063/1.4934784

[Intermolecular polarizabilities in H<sub>2</sub>-rare-gas mixtures \(H<sub>2</sub>-He, Ne, Ar, Kr, Xe\): Insight from collisional isotropic spectral properties](#)

*J. Chem. Phys.* **141**, 074315 (2014); 10.1063/1.4892864

[Morphology of collisional nonlinear spectra in H<sub>2</sub>-Kr and H<sub>2</sub>-Xe mixtures](#)

*J. Chem. Phys.* **138**, 124307 (2013); 10.1063/1.4795438

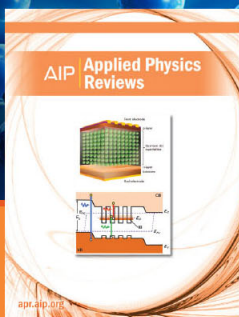
[Hyper-Rayleigh spectral intensities of gaseous Kr-Xe mixture](#)

*J. Chem. Phys.* **122**, 224323 (2005); 10.1063/1.1925267

[Investigation of the Discharge Characteristics of the T6 Hollow Cathode Operating on Several Inert Gases and a Kr/Xe Mixture](#)

*AIP Conf. Proc.* **669**, 294 (2003); 10.1063/1.1593923

---



**NEW Special Topic Sections**

**NOW ONLINE**  
Lithium Niobate Properties and Applications:  
Reviews of Emerging Trends

**AIP** | Applied Physics  
Reviews

# Anisotropic collision-induced Raman scattering by the Kr:Xe gas mixture

S. Dixneuf,<sup>1,2</sup> M. Chrysos,<sup>1,a)</sup> and F. Rachtel<sup>1</sup>

<sup>1</sup>Laboratoire des Propriétés Optiques des Matériaux et Applications, UMR CNRS 6136, Université d'Angers, 2 Boulevard Lavoisier, 49045 Angers, France

<sup>2</sup>Department of Physics, University College Cork, Cork, Ireland

(Received 25 May 2009; accepted 14 July 2009; published online 21 August 2009)

We report anisotropic collision-induced Raman scattering intensities by the Kr–Xe atomic pair recorded in a gas mixture of Kr and Xe at room temperature. We compare them to quantum-mechanical calculations on the basis of modern incremental polarizability models of either *ab initio* post-Hartree–Fock or density functional theory methods. © 2009 American Institute of Physics. [DOI: 10.1063/1.3200929]

## I. INTRODUCTION

The existence of collision-induced light scattering (CIS) by dense atomic gases has been known for over 40 yr.<sup>1–6</sup> For reasonably high gas densities, the phenomenon, albeit feeble, is well observable and can be clearly understood as the result of the variations in polarizabilities induced to pairs of gas atoms as the latter come close to each other during “collisions.” Such events are in fact nothing but short-lasting interactions, so they can only be studied effectively on the basis of a thorough understanding of spectra in the frequency representation. These spectra, so-called *binary* spectra, scale quadratically with the gas density, while they appear in the form of rather broad bands as the frequency of the scattered light gradually shifts away from the laser frequency. Once established, this density dependence can be removed therefrom, so the resulting spectrum becomes an invariant property of a single atomic pair at a given gas temperature and for the specific laser wavelength.

Physically, frequency-resolved CIS spectra are representations of differential scattering cross sections per frequency differential versus frequency shift, rather than representations of total cross sections which have units of length squared. Once normalized for gas volume, they actually become a second virial coefficient, which thus has units of volume times area per frequency differential. If frequency shift is measured in  $\text{cm}^{-1}$ , such quantities have units of length to the sixth power ( $\text{cm}^6$ ). Their use is a common practice in CIS, where they are usually referred to as the *intensity* (of the Raman spectrum of collisionally interacting pairs of atoms)  $I(\nu)$  at frequency shift  $\nu$ .

While rare gas homonuclear pairs have no interaction electric dipole, they still have some interaction polarizability. This property makes them to be CIS active even though they remain inactive in collision-induced absorption. CIS by such systems has, over the last two decades, been matter of extensive investigations, experimental and theoretical. Our group, in particular, has measured CIS signals that are extremely weak (see, for instance, Refs. 7–10). Such signals are especially relevant to the far wing of the scattering spectra and

can thus be effective probes of the very unlikely events of highly energetic collisions between gas atoms. It is only recently that a similar study was carried out for a rare gas heteronuclear pair<sup>11</sup> (Ne–Ar), soon after the publication of incremental pair-polarizability data for that system, obtained on the basis of large-scale computations as a function of interatomic distance.<sup>12,13</sup> Such findings are particularly appreciated as tools for checking whether a specific quantum chemical method is reliable enough to be used for demanding applications. This is because the atoms of a gas, unlike the atoms in a molecule, interact through van der Waals forces (as opposed to the chemical binding forces), so atomic pairs are systems far more delicate than ordinary diatomic molecules. Although some gas mixtures involving a monoatomic gas have been studied previously in CIS [for instance,  $\text{SF}_6$  and  $\text{CF}_4$  have been studied in mixtures with Ar, Kr, and Ne;<sup>14</sup>  $\text{CO}_2$  has been studied in mixture with Ar (Ref. 15)], only little is known about CIS in a mixture of two monoatomic gases.

Here, we report the first CIS results for Kr–Xe, for which *ab initio* pair-polarizability data exist only since recently.<sup>16</sup> Specifically, we give anisotropic CIS intensities by this unlike pair and by the corresponding like pairs recorded in a gas mixture of Kr and Xe at room temperature. We compare them to spectra computed quantum mechanically with data that are obtained from first principles for the anisotropy of  $(\text{Kr})_2$  (Ref. 17),  $(\text{Xe})_2$  (Ref. 18), and of Kr–Xe.<sup>16</sup> The study of an atomic mixture was an initiative born as a challenge to the topic of the traditional CIS. The choice to work with Kr–Xe was based on criteria of convenience. Kr–Xe is significantly heavier and electronically denser than Ne–Ar with a CIS distribution far more intense and sharp than the one of that system. Its detection required shorter acquisition times and produced cleaner spectra. The small experimental uncertainty was especially advantageous for our purposes, since it led to an easier extraction of the Kr–Xe spectrum out of an overall scattering signal consisting in the superimposed contributions by Kr–Xe,  $(\text{Kr})_2$ , and  $(\text{Xe})_2$ . Finally, the rich rovibrational structure of the dimer, which in lighter systems is usually insignificant at room temperature (as compared to the rototranslational envelope), was clearly observed. That structure is a good device for cross-

<sup>a)</sup>Electronic mail: michel.chrysos@univ-angers.fr.

TABLE I. HF and B3LYP anisotropy data for Kr–Xe ( $a_0^3$ ) computed by the authors with the [Kr/Xe] orbital basis set [6-311+G(3df)/9s8p7d5f] as a function of separation (bohr).

$\beta$ ( $a_0^3$ )			$\beta$ ( $a_0^3$ )		
$r$ ( $a_0$ )	HF	B3LYP	$r$ ( $a_0$ )	HF	B3LYP
6.0	8.825	10.968	12.0	1.511	1.699
6.5	7.418	9.144	12.5	1.334	1.545
7.0	6.374	7.791	13.0	1.185	1.339
7.5	5.511	6.683	13.5	1.057	1.186
8.0	4.763	5.772	14.0	0.947	1.074
8.5	4.107	4.897	14.5	0.852	0.961
9.0	3.536	4.244	15.0	0.769	0.861
9.5	3.044	3.556	16.0	0.631	0.714
10.0	2.625	3.094	17.0	0.525	0.587
10.5	2.270	2.602	18.0	0.441	0.494
11.0	1.971	2.285	19.0	0.375	0.418
11.5	1.721	1.989	20.0	0.322	0.359

checking input properties, and especially the interaction potential on which spectra of dimers are known to depend strongly.

## II. THEORETICAL

When a rare gas is irradiated by a focused laser light, the light scattered by the gas contains a weak intensity component owing to pairwise interactions. This is a binary CIS intensity lying predominately with the anisotropy of the two-body polarizability tensor. Such anisotropic intensities manifest a strong frequency dependence, exhibiting a near-exponential decrease with increasing frequency shift. Their calculation can be a difficult task especially in the wing of the spectrum where intensities are particularly weak. What reliable way to compute intensities at any frequency has been discussed in detail elsewhere.<sup>19,20</sup>

On the other hand, scattering intensities are strongly dependent on the potential of the two interacting atoms at a separation  $r$ , while they are sensitive even to small variations in the pair-polarizability anisotropy  $\beta(r)$ . Here, the most reliable representations for the Kr $\cdots$ Xe, Kr $\cdots$ Kr, and Xe $\cdots$ Xe interaction potentials were chosen, referred to as the HFDKK1 model,<sup>21</sup> the HFD-B2 model,<sup>22</sup> and the universal model,<sup>23</sup> respectively.

As the main purpose of this paper is not to study, at least on theoretical grounds, pairs of like atoms (Kr)<sub>2</sub> or (Xe)<sub>2</sub>, only representations for the Kr–Xe anisotropy will be exhaustively checked. The static anisotropy of the Kr–Xe polarizability has been calculated by Maroulis and co-workers<sup>16</sup> with two different methods. One calculation implements the perturbative second-order Møller–Plesset (MP2) theory, whereas the other implements the cost-effective B3LYP method of the density functional theory (DFT). For both, efforts have been put into diffuse orbital basis sets of near-Hartree–Fock (HF) quality, referred to as [8s7p6d5f] (Ref. 17) and B3=[9s8p7d5f] (Ref. 18) for krypton and xenon, respectively. We also calculated and report below a new B3LYP model for Kr–Xe using Pople’s [6-311+G(3df)] (Ref. 24) and Maroulis’s B3 (Ref. 18) basis sets for krypton and xenon, respectively. The data of that

model are given in Table I for several values of separation starting from the value  $r=6$  bohr, which corresponds to the closest approach between Kr and Xe effectively probed by CIS at the working temperature.

As for (Kr)<sub>2</sub> and (Xe)<sub>2</sub>, polarizability invariants that are obtained rigorously from first principles are of particular interest, even if only static. These again are models obtained by Maroulis. They were computed with the self-consistent field (SCF) or the MP2 method<sup>17</sup> as regards krypton and with B3LYP or MP2 (Ref. 18) as regards xenon for the respective above-mentioned basis sets. For every quantum-chemistry calculation, the basis set superposition error has been accounted for through the well-tested Boys–Bernardi counterpoise-correction approach. No relativistic corrections have been considered. Since data on Cauchy moments are only fragmentary, no frequency correction to the anisotropy was considered at the laser frequency.<sup>25,26</sup> Henceforth, anisotropy is considered to be static and so are the models that we used to calculate spectra.

To extrapolate beyond the range of the anisotropy data now available, the well-known long-range dipole-induced dipole model was used. Values for the atomic polarizabilities for krypton  $\alpha_{\text{Kr}}$  and for xenon  $\alpha_{\text{Xe}}$  needed in that asymptotic model are given in Table II.<sup>17,18</sup>

Anisotropy representations for Kr–Xe are illustrated in Fig. 1 along with the properties for the two like pairs. In order for the comparison to be meaningful, only MP2 is shown for the latter two systems. Thus, anisotropy functions computed at least at one same *ab initio* level for all the three

TABLE II. Static polarizabilities ( $a_0^3$ ) for Kr,  $\alpha_{\text{Kr}}$  and for Xe,  $\alpha_{\text{Xe}}$  computed with various methods.

	SCF	MP2	B3LYP	HF
Kr	16.45 <sup>a</sup>		17.066 <sup>b</sup>	16.058 <sup>b</sup>
Xe	27.05 <sup>a</sup>	27.71 <sup>a</sup>	28.44 <sup>a</sup> 28.422 <sup>b</sup>	27.027 <sup>b</sup>

<sup>a</sup>[Kr/Xe] orbital basis set used: [8s7p6d5f/9s8p7d5f] (Ref. 16).

<sup>b</sup>[Kr/Xe] orbital basis set used: [6-311+G(3df)/9s8p7d5f] (this work).

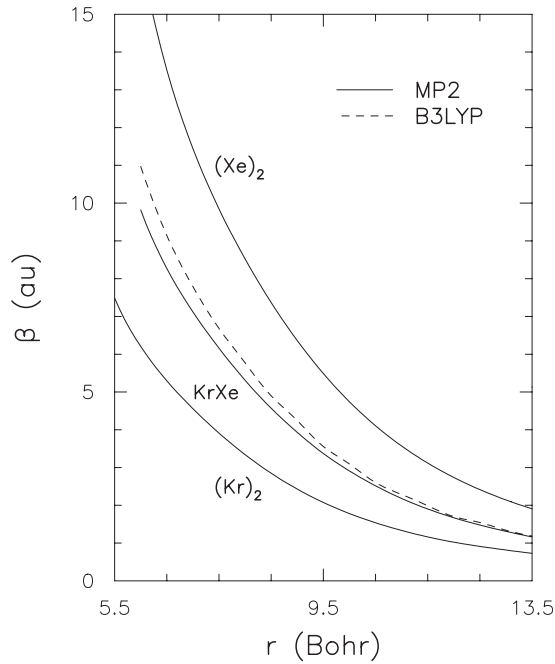


FIG. 1. Kr–Xe anisotropy representations ( $a_0^3$ ) computed with MP2 and B3LYP theory as a function of interatomic separation (bohr) (Ref. 16). The MP2 models for  $(\text{Kr})_2$  (Ref. 17) and  $(\text{Xe})_2$  (Ref. 18) are also shown for comparison.

pairs can be compared. The starting  $r$  value in each of the plotted anisotropy curves corresponds to the closest separation that was effectively probed with CIS at the working temperature, i.e.,  $r \approx 6.25$ , 6, and 5.5 bohr for  $(\text{Xe})_2$ , Kr–Xe, and  $(\text{Kr})_2$ , respectively.

Analogous to what has been found to occur in other atomic mixtures,<sup>11</sup> the anisotropy curves of Kr–Xe lie between the ones of the two like pairs. The anisotropy of Kr–Xe, unlike that of Ne–Ar, does not seem to mimic singularly the anisotropy shape of any like pair. This is because unlike  $(\text{Ne})_2$  and  $(\text{Ar})_2$ , the heavy  $(\text{Kr})_2$  and  $(\text{Xe})_2$  exhibit anisotropies with a similar though quantitatively distinct shape.<sup>11</sup> As has already been observed by Maroulis for other rare gas pairs, DFT has a more marked response than have *ab initio* computations for the anisotropy, even though in the present case the discrepancy between B3LYP and MP2 is smaller than was found to be in Ne–Ar.<sup>12</sup> The fact that increase in the atomic size tends to reduce the discrepancy between the rather simple variational B3LYP model and the large-scale *ab initio* computations suggests that DFT is an interesting alternative when dealing with systems of high electronic density.

Finally, our B3LYP model for Kr–Xe was found to be indistinguishable from Maroulis’s B3LYP calculation, which suggests that at least at this level of theory the extended basis set he has proposed for krypton (the only point differentiating the two calculations) is not critical for the anisotropy.

### III. EXPERIMENTAL

Scattering photon signals were produced, recorded, and processed by a high sensitivity right-angle Raman scattering setup. A detailed description can be found in Ref. 10. The incident wave was delivered by a continuous ion-argon laser

with output wavelength  $\lambda_L = 514.5$  nm, which is a green wavelength. To spectrally disperse the scattered light, a double monochromator with two 1800 grooves/mm holographic gratings was used. Among the two detection chains available in the setup, we only needed the single-channel one consisting of a photomultiplier, of an amplifier, of a discriminator, and of a photon counter over the spectral range covered. In order to make it possible to record the anisotropic signal component  $I_{\parallel}$ , the incident field polarization was forced into the direction ( $\parallel$ ) of the scattered beam wave vector. Calibration of the binary signal on an absolute intensity scale was made by reference to the integrated intensity of the  $S_0(0)$  rotational line of molecular hydrogen.<sup>10,11</sup>

For the study in mixture, what we were interested in was absolute-unit anisotropic intensities by the unlike pair  $I_{\text{KrXe}}$  as a function of frequency shift  $\nu$ . (Henceforth, index  $\parallel$  is dropped for the sake of notational convenience.) A specific procedure was followed to isolate at each frequency shift  $\nu$ , the intensity  $I_{\text{KrXe}}$  from the recorded noise-corrected binary scattering signal  $S_{(2)}(\nu)$ . This procedure goes in two steps. The first step is to mathematically define  $S_{(2)}(\nu)$ . Owing to the binary nature of the interactions, this quantity reads

$$S_{(2)} = \frac{\rho_{\text{Kr}}^2}{2!} I_{\text{KrKr}} + \rho_{\text{Kr}} \rho_{\text{Xe}} I_{\text{KrXe}} + \frac{\rho_{\text{Xe}}^2}{2!} I_{\text{XeXe}}, \quad (1)$$

where  $I_{\text{KrKr}}$  and  $I_{\text{XeXe}}$  denote the absolute-unit anisotropic intensities by the corresponding like pairs and  $\rho_{\text{Kr}}$  and  $\rho_{\text{Xe}}$  are the partial densities (in amagat) of the two gases, respectively. In this expression, the three intensities  $I_{\text{KrKr}}$ ,  $I_{\text{XeXe}}$ , and  $I_{\text{KrXe}}$  are, respectively, weighted by  $\rho_{\text{Kr}}^2/2!$ ,  $\rho_{\text{Xe}}^2/2!$ , and  $\rho_{\text{Kr}}\rho_{\text{Xe}}$ , that is, by the number density of the two like atomic pairs in the mixture and by the number density of the unlike pairs. The second step is to extract at each frequency shift  $\nu$  the quantity  $I_{\text{KrXe}}$  from the mother absolute-unit overall binary intensity  $I_{(2)}(\nu) = S_{(2)}(\nu) / \rho_{\text{Kr}}\rho_{\text{Xe}}$ . Mathematically, this step is summarized as follows:

$$I_{\text{KrXe}}(\nu) = I_{(2)}(\nu) - \frac{1}{2} \gamma I_{\text{KrKr}}(\nu) - \frac{1}{2} \gamma^{-1} I_{\text{XeXe}}(\nu), \quad (2)$$

with  $\gamma = \rho_{\text{Kr}}/\rho_{\text{Xe}}$  as the partial density ratio of the mixed gases chosen to be unity all along the study.

In order to extract intensities solely binary from the total recorded signal, a careful study was made with varying gas density. Density variations were considered within ranges depending on the gas. Optimal working ranges were [2:40], [2:30], and [5:60] amagat for pure krypton, for pure xenon, and for their mixture, respectively, with gas density being of course an additive property. The density of the mixture was steadily decreased with  $\nu$  in such a way that only binary interactions contributed to the recorded intensities.

Run pressure in atmosphere units was converted to density (amagat) using the second-order virial equation of state, known to be the most interesting and versatile of the equations of state for gases.<sup>27</sup> Values for the second and third virial coefficients for krypton,<sup>28</sup> for xenon,<sup>29</sup> and for their mixture,<sup>30,31</sup>  $B_{\text{KrKr}} = -51.8434$  cm<sup>3</sup> mol<sup>-1</sup>,  $C_{\text{KrKrKr}} = 2265.57$  cm<sup>6</sup> mol<sup>-2</sup>,  $B_{\text{XeXe}} = -133.455$  cm<sup>3</sup> mol<sup>-1</sup>,  $C_{\text{XeXeXe}} = 5771.71$  cm<sup>6</sup> mol<sup>-2</sup>, and  $B_{\text{KrXe}} = -80.4167$  cm<sup>3</sup> mol<sup>-1</sup>, were deduced by interpolating the most appropriate physical

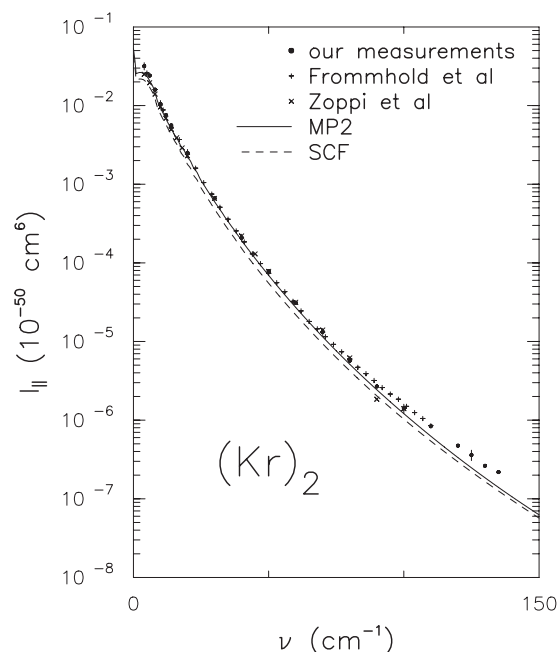


FIG. 2. Absolute-unit anisotropic CIS spectrum  $I_{\text{KrKr}}$  ( $\text{cm}^6$ ) as a function of frequency shift ( $\text{cm}^{-1}$ ). Our data ( $\bullet$ ) are compared to past experiments ( $+$ ) (Ref. 32) and ( $\times$ ) (Ref. 33) and to quantum-mechanical intensities from the MP2 and the SCF ( $\text{Kr}$ )<sub>2</sub> anisotropy models of Ref. 17.

vapor transport data available at the temperature of the experiment,  $T=294.5$  K. The second virial coefficient of the mixture was taken as a specific linear combination of  $B_{\text{KrKr}}$ ,  $B_{\text{XeXe}}$ , and  $B_{\text{KrXe}}$ , while the third virial coefficient was taken as the geometric mean of  $C_{\text{KrKrKr}}$  and  $C_{\text{XeXeXe}}$ .<sup>11,27</sup>

#### IV. RESULTS

Given the interaction potential and the polarizability anisotropy models, line shapes were calculated by using reliable numerical methods developed in our group.<sup>19,20</sup> Figures 2 and 3 illustrate, as a function of frequency shift, absolute-unit anisotropic intensities  $I_{\text{KrKr}}$  and  $I_{\text{XeXe}}$  recorded over the range  $[4:135]$   $\text{cm}^{-1}$  and  $[4:130]$   $\text{cm}^{-1}$ , respectively. Experimental intensities and uncertainties are given in Table III. As expected from a heavy gas, scattering intensities at low frequency shift are higher than the ones by lighter gases. On the other hand, they fall off with increasing frequency much more quickly than they do in lighter systems, covering some six orders of magnitude over 135  $\text{cm}^{-1}$ . Our measurements were compared to the previous measurements by Frommhold and co-workers<sup>32</sup> and Zoppi *et al.*,<sup>33</sup> and also to spectra computed quantum mechanically from anisotropy data by Maroulis. We remind the reader that these data for ( $\text{Kr}$ )<sub>2</sub> have been obtained exclusively *ab initio* on the basis of the SCF or the MP2 methods;<sup>17</sup> For ( $\text{Xe}$ )<sub>2</sub>, they have been obtained with MP2 or in a non-*ab initio* way using the B3LYP functional.<sup>18</sup> Our measurements appear consistent with the former experiments with maximum discrepancies smaller than 10% and 15% for krypton and xenon, respectively, all lying within the experimental errors. They also covered for krypton and xenon the hitherto undescribed spectral ranges  $[110:135]$   $\text{cm}^{-1}$  (Refs. 32 and 33) and  $[4:8] \cup [116:130]$   $\text{cm}^{-1}$ ,<sup>32</sup> respectively.

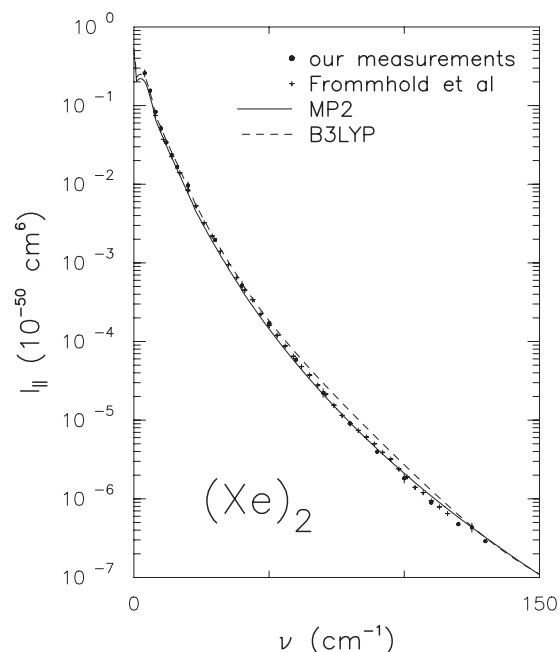


FIG. 3. Absolute-unit anisotropic CIS spectrum  $I_{\text{XeXe}}$  ( $\text{cm}^6$ ) as a function of frequency shift ( $\text{cm}^{-1}$ ). Our data ( $\bullet$ ) are compared to a past experiment ( $+$ ) (Ref. 32) and to quantum-mechanical intensities from the MP2 and the B3LYP ( $\text{Xe}$ )<sub>2</sub> anisotropy models of Ref. 18.

As already observed for most of the monoatomic gases previously studied, inclusion of dynamic electron correlation clearly optimizes pair anisotropy. This is indeed the case with krypton shown in Fig. 2 and even more with xenon shown in Fig. 3. There, MP2 appears as a valuable representation of the anisotropy for each of these systems even though it steadily underestimates the scattering intensities for the former one. SCF calculations, which unlike MP2 completely disregard dynamic electron correlation, provided ( $\text{Kr}$ )<sub>2</sub> intensities by 20% below the experiment at medium frequency shift and by 43% at 135  $\text{cm}^{-1}$ . As clearly illustrated in Fig. 3, there is a striking agreement between the MP2 theory and our measurements for ( $\text{Xe}$ )<sub>2</sub> with a calculated spectrum lying everywhere within the limits of experimental uncertainty. Calculations in this study like in a parallel study<sup>11</sup> showed that this is not the case with DFT, which provides overestimating predictions with, in the present case, a maximum discrepancy of 43% at 80  $\text{cm}^{-1}$ .

The absolute-unit anisotropic scattering intensity of  $\text{Kr-Xe}$  is plotted on Fig. 4 as a function of frequency shift. Values of the intensities are given in Table III. Experimentally, the  $\text{Kr-Xe}$  photon signal could be extracted over the range  $[4:130]$   $\text{cm}^{-1}$ . We emphasize the low dispersion of our data, given that each of the points was obtained through a difficult procedure of extraction implementing processing and subtraction of several coexisting signals. At frequency shifts that are below  $\approx 30$   $\text{cm}^{-1}$ , the intensity of  $\text{Kr-Xe}$  lies in between the intensities of the two like pairs. As  $\nu$  is increased further, intensities that are comparable to or even slightly higher than the intensities of ( $\text{Kr}$ )<sub>2</sub> and ( $\text{Xe}$ )<sub>2</sub> are obtained. A similar trend can be observed in  $\text{SF}_6\text{-Kr}$ . The intensity of this mixture below  $\approx 15$   $\text{cm}^{-1}$  is between the intensity of  $\text{SF}_6\text{-SF}_6$  and that of ( $\text{Kr}$ )<sub>2</sub>, whereas it slightly exceeds both those intensities in the wing.<sup>14</sup>

TABLE III. Absolute-unit anisotropic scattering intensities ( $\text{cm}^6$ ) recorded by pure gaseous krypton  $I_{\text{KrKr}}$  or xenon  $I_{\text{XeXe}}$  and by their mixture  $I_{\text{KrXe}}$  as a function of frequency shift  $\nu$  ( $\text{cm}^{-1}$ ).

$\nu$ ( $\text{cm}^{-1}$ )	$I_{\text{KrKr}}$ ( $\text{cm}^6$ )	$I_{\text{XeXe}}$ ( $\text{cm}^6$ )	$I_{\text{KrXe}}$ ( $\text{cm}^6$ )
4	$3.17 \times 10^{-52} \pm 11\%$	$2.59 \times 10^{-51} \pm 11\%$	$7.32 \times 10^{-52} \pm 22\%$
6	$2.41 \times 10^{-52}$	$1.55 \times 10^{-51}$	$5.27 \times 10^{-52}$
8	$1.59 \times 10^{-52}$	$8.34 \times 10^{-52}$	$3.09 \times 10^{-52}$
10	$1.05 \times 10^{-52} \pm 11\%$	$5.10 \times 10^{-52} \pm 11\%$	$1.96 \times 10^{-52} \pm 22\%$
12	$7.61 \times 10^{-53}$	$3.40 \times 10^{-52}$	$1.36 \times 10^{-52}$
14	$5.61 \times 10^{-53}$	$2.36 \times 10^{-52}$	$9.45 \times 10^{-53}$
20	$2.50 \times 10^{-53} \pm 11\%$	$9.65 \times 10^{-53} \pm 11\%$	$5.26 \times 10^{-53} \pm 22\%$
30	$6.61 \times 10^{-54}$	$1.96 \times 10^{-53}$	$1.32 \times 10^{-53}$
40	$2.09 \times 10^{-54} \pm 11\%$	$5.15 \times 10^{-54} \pm 13\%$	$3.78 \times 10^{-54} \pm 22\%$
50	$7.86 \times 10^{-55}$	$1.71 \times 10^{-54}$	$1.23 \times 10^{-54}$
60	$3.12 \times 10^{-55}$	$5.89 \times 10^{-55}$	$5.08 \times 10^{-55}$
70	$1.33 \times 10^{-55} \pm 11\%$	$2.23 \times 10^{-55} \pm 13\%$	$2.22 \times 10^{-55} \pm 22\%$
80	$5.70 \times 10^{-56}$	$9.10 \times 10^{-56}$	$7.96 \times 10^{-56}$
90	$2.68 \times 10^{-56}$	$3.99 \times 10^{-56}$	$3.38 \times 10^{-56}$
100	$1.41 \times 10^{-56} \pm 13\%$	$1.83 \times 10^{-56} \pm 13\%$	$2.18 \times 10^{-56} \pm 32\%$
110	$8.39 \times 10^{-57}$	$8.97 \times 10^{-57}$	$1.79 \times 10^{-56}$
120	$4.74 \times 10^{-57}$	$4.75 \times 10^{-57}$	$1.16 \times 10^{-56}$
125	$3.61 \times 10^{-57} \pm 15\%$	$4.34 \times 10^{-57} \pm 13\%$	$9.47 \times 10^{-57} \pm 32\%$
130	$2.63 \times 10^{-57}$	$2.89 \times 10^{-57}$	$5.98 \times 10^{-57}$
135	$2.19 \times 10^{-57}$		

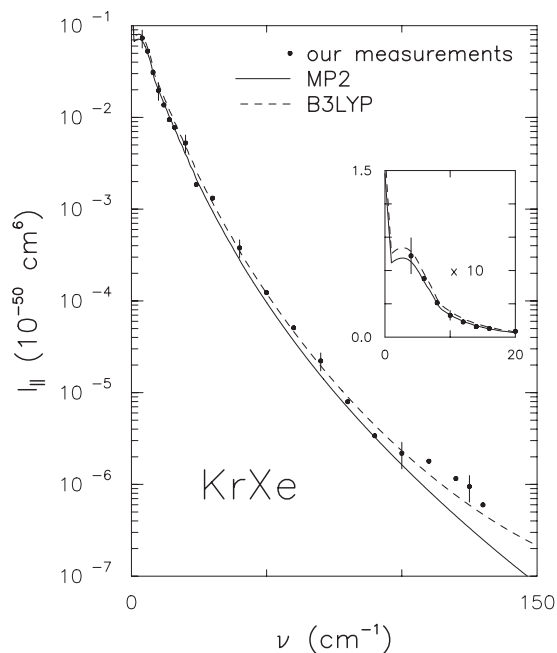


FIG. 4. Absolute-unit anisotropic CIS spectrum  $I_{\text{KrXe}}$  ( $\text{cm}^6$ ) as a function of frequency shift ( $\text{cm}^{-1}$ ). Quantum-mechanical intensities computed with the Kr–Xe anisotropy models of Fig. 1 are also shown for comparison. The B3LYP model computed by the authors with the [6-311+G(3df)/9s8p7d5f] orbital basis set provided a spectrum that was indistinguishable from the spectrum computed with the B3LYP model of Haskopoulos *et al.* (Ref. 16). The domain [0:20]  $\text{cm}^{-1}$  was enhanced in the inset in order to highlight the contribution of the bound and predissociating KrXe dimers. A slit function of 1  $\text{cm}^{-1}$  width at half maximum was taken to mimic the aperture used.

As expected for heavy gases, stable and predissociating<sup>34</sup> KrXe dimers have a large contribution to the scattering intensity at low frequency shift, which, as shown in the inset expanding that region, were clearly observed below 8  $\text{cm}^{-1}$ . According to our calculations, rotational states with angular momenta as large as  $J=127$  are populated in KrXe.

When focusing on theory, MP2 intensities by Kr–Xe perfectly reproduce the observation below 25  $\text{cm}^{-1}$ , keeping within the experimental errors up to 100  $\text{cm}^{-1}$ . Beyond that value, it is the DFT description which agrees the best with the experiment in a way analogous to findings for Ne–Ar.<sup>11</sup> A better inclusion of dynamic electron correlation, presumably on the basis of some coupled-cluster level of optimization, should be expected to describe better the anisotropy close to the unified atom limit so that the spectrum wing rises in intensity.<sup>35</sup>

Table IV allows one to compare the theory with experiment on the basis of zeroth-order, first-order, second-order, third-order, and fourth-order spectral moments. Given the quantum treatment here offered, odd-order moments are not zero, even in the near classical system at hand. Our findings confirm that MP2 theory does indeed describe a reality at low frequency shift, which is the range contributing mainly to  $M_0$ .

Finally, from the measured  $M_0$  we were able to provide the estimate  $B_K = 6.74 \times 10^{-11} \pm 1.35 \text{ cm}^9 \text{ erg}^{-1} \text{ mol}^{-2}$  for the Kerr second virial coefficient. This was done within the approximation  $B_K^{(0)} \approx B_K^{(0)\alpha^2}$ ,<sup>36</sup> which for heavy gases is expected to be almost an exact result (see, for instance, Table III of Ref. 37).

TABLE IV.  $n$ th-order anisotropic spectral moments ( $\text{\AA}^n \text{s}^{-n}$ ) for Kr–Xe.

This work	$M_0$ ( $10^2 \text{\AA}^0$ )	$M_1$ ( $10^{13} \text{\AA}^1 \text{s}^{-1}$ )	$M_2$ ( $10^{27} \text{\AA}^2 \text{s}^{-2}$ )	$M_3$ ( $10^{38} \text{\AA}^3 \text{s}^{-3}$ )	$M_4$ ( $10^{52} \text{\AA}^4 \text{s}^{-4}$ )
Expt.	$4.87 \pm 20\%$	$1.91 \pm 20\%$	$1.48 \pm 20\%$	$6.08 \pm 25\%$	$4.95 \pm 30\%$
MP2 <sup>a</sup>	4.60	1.69	1.30	4.84	3.77
B3LYP <sup>b</sup>	5.26	2.03	1.57	7.59	$\geq 6.04$

<sup>a</sup>Spectral moments calculated by the authors with data taken from Ref. 16.<sup>b</sup>This work.

## V. SYNOPSIS

This paper reports the first data in the CIS literature for Kr–Xe. Such a heavy pair of unlike rare gas atoms is, for a multitude of structural characteristics, a challenging system for both theory and experiment. We carried out an exhaustive joint experimental/theoretical study of the Kr:Xe gas mixture at room temperature and for total density varying from 5 to 60 amagat. Frequency-resolved intensities were measured over a range of frequency shift going far into the wing of a rapidly falling spectrum. According to our findings, MP2 theory was found to describe quite consistently the observation, except in the spectrum wing where relativistic effects, unaccounted for, are expected to be significant. Same conclusion was drawn as to an anisotropy representation computed by the authors on the level of DFT. Striking agreement was seen at the low values of frequency shift where bound and resonance states of stable and predissociating KrXe dimers were shown to have a substantial contribution. This observation adds credibility to the interaction potentials used for the three systems involved in the analysis. The overall good agreement between theory and experiment once again lends credence to the delicate procedure to subtract signals, which had so far been seemingly the major obstacle for CIS experiments with atomic gas mixtures. The limitation of the MP2 in the wing of the spectrum should be interpreted in part as being due to relativistic phenomena neglected in the calculations. To what extent a relativistic *ab initio* calculation would affect the anisotropy of the three systems involved in this study is an open question. Whatever the influence these or other missing effects might have on CIS spectra, DFT can still be regarded as an affordable alternative to expensive *ab initio* computations for electronically dense rare gas atomic pairs.

<sup>1</sup>J. P. C. McTague and G. Birnbaum, *Phys. Rev. Lett.* **21**, 661 (1968).<sup>2</sup>M. H. Proffitt and L. Frommhold, *Phys. Rev. Lett.* **42**, 1473 (1979).<sup>3</sup>L. Frommhold and M. H. Proffitt, *Phys. Rev. A* **21**, 1249 (1980).<sup>4</sup>L. Frommhold, *Adv. Chem. Phys.* **46**, 1 (1981).<sup>5</sup>A. Borysov and L. Frommhold, *Adv. Chem. Phys.* **75**, 439 (1989).<sup>6</sup>*Collision- and Interaction-Induced Spectroscopy*, NATO ASI Series C: Mathematical and Physical Sciences Vol. 452, edited by G. C. Tabisz and M. N. Neuman (Kluwer, Dordrecht, 1995).<sup>7</sup>F. Chapeau-Blondeau, V. Teboul, J. Berru , and Y. Le Duff, *Phys. Lett. A* **173**, 153 (1993).<sup>8</sup>O. Gaye, M. Chrysos, V. Teboul, and Y. Le Duff, *Phys. Rev. A* **55**, 3484 (1997).<sup>9</sup>F. Rachet, M. Chrysos, C. Guillot-No l, and Y. Le Duff, *Phys. Rev. Lett.* **84**, 2120 (2000).<sup>10</sup>F. Rachet, Y. Le Duff, C. Guillot-No l, and M. Chrysos, *Phys. Rev. A* **61**, 062501 (2000).<sup>11</sup>S. Dixneuf, M. Chrysos, and F. Rachet *Phys. Rev. A* **80**, 022703 (2009).<sup>12</sup>G. Maroulis and A. Haskopoulos, *Chem. Phys. Lett.* **358**, 64 (2002).<sup>13</sup>J. L. Cacheiro, B. Fern ndez, D. Marchesan, S. Coriani, C. H ttig, and A. Rizzo, *Mol. Phys.* **102**, 101 (2004).<sup>14</sup>S. M. El-Sheikh and G. C. Tabisz, *Mol. Phys.* **68**, 1225 (1989).<sup>15</sup>M. Chrysos, F. Rachet, N. I. Egorova, and A. P. Kouzov, *Phys. Rev. A* **75**, 012707 (2007).<sup>16</sup>A. Haskopoulos, D. Xenides, and G. Maroulis, *Chem. Phys.* **309**, 271 (2005).<sup>17</sup>G. Maroulis, *J. Phys. Chem. A* **104**, 4772 (2000).<sup>18</sup>G. Maroulis, A. Haskopoulos, and D. Xenides, *Chem. Phys. Lett.* **396**, 59 (2004).<sup>19</sup>M. Chrysos, O. Gaye, and Y. Le Duff, *J. Chem. Phys.* **105**, 31 (1996).<sup>20</sup>M. Chrysos, O. Gaye, and Y. Le Duff, *J. Phys. B* **29**, 583 (1996).<sup>21</sup>R. A. Aziz and A. van Dalen, *J. Chem. Phys.* **78**, 2402 (1983).<sup>22</sup>A. K. Dham, A. R. Allnatt, and W. J. Meath, *Mol. Phys.* **67**, 1291 (1989).<sup>23</sup>A. D. Koutselos, E. A. Mason, and L. A. Viehland, *J. Chem. Phys.* **93**, 7125 (1990).<sup>24</sup>W. J. Hehre, L. Radom, P. R. Schleyer, and J. A. Pople, *Ab Initio Molecular Orbital Theory* (Wiley, New York, 1986).<sup>25</sup>B. Fern ndez, C. H ttig, H. Koch, and A. Rizzo, *J. Chem. Phys.* **110**, 2872 (1999).<sup>26</sup>C. H ttig, H. Larsen, J. Olsen, P. Jorgensen, H. Koch, B. Fern ndez, and A. Rizzo, *J. Chem. Phys.* **111**, 10099 (1999).<sup>27</sup>J. H. Dymond and E. B. Smith, *The Virial Coefficients of Pure Gases and Mixtures: A Critical Compilation* (Oxford University Press, New York, 1980).<sup>28</sup>N. J. Trappeniers, T. Wassenaar, and G. J. Wolkers, *Physica* **32**, 1503 (1966).<sup>29</sup>A. Michels, T. Wassenaar, and P. Louwerse, *Physica* **20**, 99 (1954).<sup>30</sup>C. A. Pollard and G. Saville, *The Virial Coefficients of Pure Gases and Mixtures: A Critical Compilation* (Ref. 27), p. 469.<sup>31</sup>B. Schramm, H. Schmiedel, R. Gehrman, and R. Bartl, *Ber. Bunsenges. Phys. Chem.* **81**, 316 (1977).<sup>32</sup>M. H. Proffitt, J. W. Keto, and L. Frommhold, *Can. J. Phys.* **59**, 1459 (1981).<sup>33</sup>M. Zoppi, M. Moraldi, F. Barocchi, R. Magli, and U. Bafile, *Chem. Phys. Lett.* **83**, 294 (1981).<sup>34</sup>The term ‘‘predissociating dimers’’ refers to the predissociating states of the KrXe dimer, which are scattering resonances. It is preferable, in the context of this paper, to use this particular term rather than the term ‘‘metastable dimers,’’ which, although occasionally employed in the CIS literature, is originally (and properly) used for electronic states.<sup>35</sup>According to other observations in a variety of atomic pairs, the more electron correlation is included the more the wing of the spectrum is intense, provided that *ab initio* methods of high optimization level are compared. In this respect, the increase in the wing appears in the same order as the order of appearance of the following response approaches: MP2, CCSD, and CCSD(T), which are the three *ab initio* approaches most often used to model polarizabilities of atomic pairs.<sup>36</sup>By using the notations of Ref. 37.<sup>37</sup>A. Rizzo, S. Coriani, D. Marchesan, J. L. Cacheiro, B. Fern ndez, and C. H ttig, *Mol. Phys.* **104**, 305 (2006).